Residual Stress Estimation of Welded Tubular K-joints under Fatigue Loads

C. Acevedo[1], A. Nussbaumer [1]
[1]*Swiss Federal Institute of Technology, Lausanne, Switzerland*

ABSTRACT

In tubular joints, the hot spot stress concept is used to characterize the stress field at potential fatigue crack locations. The combination of determining stresses using the hot spot concept, with a reduction factor on fatigue strength is however not a satisfactory solution. In this paper, an overview of a on-going research project in which the overall phenomenon, including geometrical size effects, welding residual stresses and loading effects, is presented.
Within this project, fatigue tests and residual stresses investigations are carried out on planar circular hollow sections (CHS) truss girders as well as on isolated K-joints. Residual stresses measurements aim to get intensity, variability with depth and influence of fabrication sequence. They are obtained using the incremental hole-drilling method.

1 INTRODUCTION

Residual stresses were defined by Gurney in 1979 [1] as "locked-in stresses that exist in a body or a part of a body in the absence of any externally applied load". In practice, these internal self-balanced stresses can be introduced in materials or components during different manufacturing processes (mechanical treatment, heat treatment, machining, welding, etc.). The weld vicinity is not only the area where the highest tensile residual stress can be found, but also where local stress concentrations due to geometric discontinuities have occurred and where metallurgical discontinuities (inclusions, undercut, etc.) have been left by the welding process. Tensile residual stresses suppress crack closure thus increasing crack propagation rate. This is particularly true for tubular bridges, in which the fatigue performance of the welded joints is critical for the bridge design.
In order to take into account the effects of residual stresses on fatigue design, it is important to have high-quality measurement methods. In this paper, the hole-drilling method is presented with applications on tubular joints. A specific hole-drilling support system has been developed for measurements on tubes. First results achieved are analysed.

2 LITERATURE REVIEW: RESIDUAL STRESS IN WELDED TUBULAR JOINTS

To improve failure predictions, the American and European defect assessment procedures of pressure vessel and piping components, have made progress in weld residual stress estimates during the last decade, their developments were reported in API 579 Appendix E [2] and in BS 7910:1999 of the SINTAP project [3]. The objectives were to complete the earlier investigation of residual stress data.

A number of measurements of the residual stresses in tubular joints due to the welding process were undertaken by researchers at Cambridge University in the 1980s. In Payne & Porter Goff 1985 [3], measurements on three welded tubular T-joint specimens are described. These specimens consisted of tubes ranging 610-455x11-16 mm brace members welded to 915x22-36 mm chord members using a metal inert gas (MIG) process with a heat input of about 600 J/mm per pass. In Porter Goff et al. 1988 [4], similar measurements on two welded tubular Y-joint and three welded pipe-to-endplate specimens are described.

One of the major conclusions of the research carried out at Cambridge University was that the mean longitudinal stresses (stresses parallel to the weld direction) obtained by sectioning never exceeded the material yield stress, f_y, by more than 20 N/mm^2. Furthermore, mean transverse residual stresses were never seen to exceed ~0.65·fy. In general, it is the transverse stress distribution that is of the most interest, as the principal stresses due to the applied loads also tend to be oriented perpendicularly (or transversely) to the weld direction.

In Stacey et al. 2000 [5], measured residual stress data are presented for a number of details applicable to tubular structures including: T-butt joints, pipe-to-endplate joints, tubular T-, and Y-joints. Stacey proposed residual stress distributions to model the residual stress due to welding in tubular joints.

It has to be noticed that these investigations generally deal with pipes or pressure vessels thin cylinders with diameters ranging between 600 and 1000 mm, whereas tubes in bridges are often thick cylinders with diameters lower than 600 mm.

3 FATIGUE TEST

The test specimens are uni-planar tubular CHS welded truss beams, 9 m in length and 2 m in height, tested under fatigue loading (see Figure 1). Four series using similar specimens were tested in total by Schumacher [6] and Borges [7]. Truss members are made of structural steel with a nominal yield strength of $355N/mm^2$. The test set-up static system corresponded to a simple beam with a concentrated load at mid-span. The fatigue test consisted of sinusoidal fatigue load, applied at a frequency of about 0.7 Hz, with a load ratio $R = Q_{min}/Q_{max}$ of $R = 0.1$.

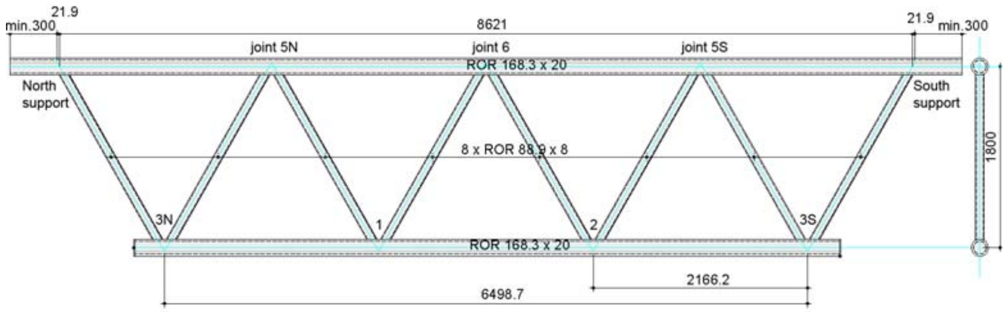

Figure 1: Elevation of a truss beam with dimensions and joint numbering

The test results are expressed in the form of hot-spot stress range, $S_{r,hs}$, versus number of cycles, N. In order to compare the results, one has to define a coherent definition of joint failure. Here, all results are expressed as the life corresponding to complete loss of strength of the joint and identified as N_4. Figure 2 shows the results of these tests, together with those of previous similar tests and those from the existing IIW database [8] on CHS joints. The size of the symbols is proportional to the chord thickness, T.

Our data shows on the graph as only 14 points, but in fact represents 22 fatigue cracks. More precisely, looking at the series S5 (beams S5-1 and S5-2), fatigue cracks were obtained in different joints j1, j2, j5N, j5S (see Figure 1), located on the tension chord but also on the compression chord. This fact could be explained by the presence of residual stresses in the weld toe vicinity. All the cracks occurred at hot-spots 1 or 1c (side of brace in compression in the case of chord in compression); for hot spot locations, see Figure 3. It was observed that crack growth, at least up to half the chord thickness, occurred at about the same rate both in tension or compression joints, with crack shapes (a/c) being also similar. However, crack angles seem to be lower in compression joints than in tension joints.

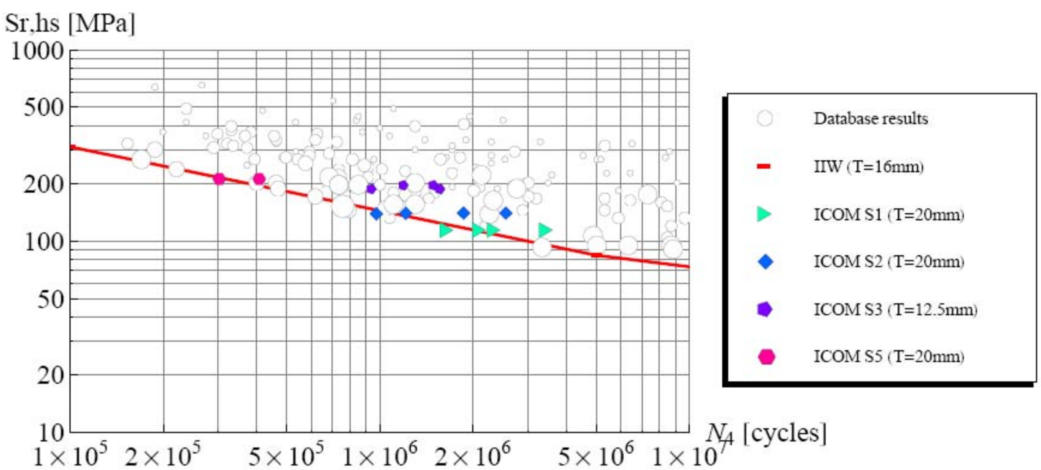

Figure 2: S-N test results on CHS joints

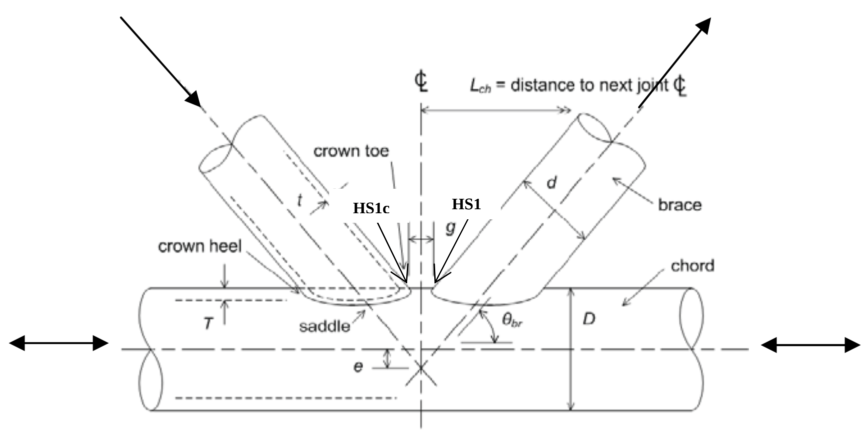

Figure 3: Hot-spot locations on a CHS joint

4 HOLE DRILLING INSTRUMENTATION FOR WELDED TUBULAR K-JOINTS

The principle of the Hole-Drilling method was first proposed by Mathar in 1934 [9]. From 1950 until now, the accuracy of the procedure has been greatly improved, and in 1981, it has been standardised in ASTM Standard Test Method E837. In this paper, we have referred to the last updated version ASTM E837-08 [10].

This method is based on the stress relaxation induced by the drilling of a small hole: generally 1-5 mm in diameter and a depth approximately equal to its diameter. As illustrated in Figure 4, strain-gauge rosettes, glued around the hole before drilling, measure the relieved surface strains. Thus, from these relieved strains, it is possible to calculate the residual stress field present in the material before the hole was drilled.

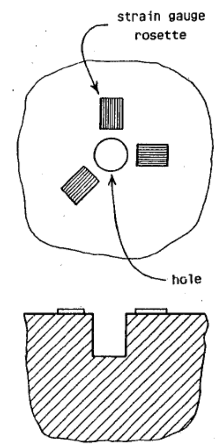

Figure 4:Hole drilling principle[11]

This method is often defined as a semi-destructive method because the material is locally removed and the residual stresses are relaxed in a limited area. As a consequence, the residual field is only estimated near the surface.

In this method, strains are measured by means of rosette composed of three strain-gauge grids with a special direction each. As shown in Figure 5, the direction of gauge 1 is the reference direction (the x-axis), gauge 2 is 45° or 135° clockwise of the reference and gauge 3 is 90° clockwise of the reference.

Three strain-gauges are needed in order to evaluate the values of the three originally in-plane stresses σ_x, σ_y and τ_{xy}, or to evaluate the principal stresses σ_{min},σ_{max} and β, the angle between the x-axis and the direction of σ_{max}.

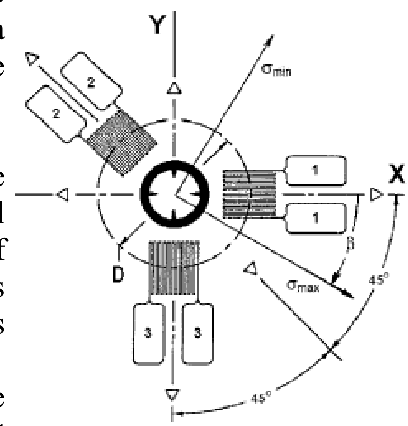

Figure 5: Strain gauge rosette[10]

The principle of this method is based on several assumptions:

- **The material is homogeneous isotropic linear-elastic**. Thus, if local yielding reaches and exceeds 60% of the material yield stress, which could be the case of large weld-induced residual stress, the accuracy of the measurement will decrease.
- **The stress state is a plane stress state in xy plane**
- **Stresses are uniform throughout the hole depth**. However, stresses could be non-uniform through the full thickness of the material.
- **No additional stresses are induced by the drilling** (no local yielding, no overheating).

The relationship (Eq.1) between the residual stresses present in the material before the hole was drilled, and the relaxed surface strains ε by the hole-drilling is as follows:

$$\varepsilon = \frac{1+\nu}{E} \cdot \bar{a} \cdot \frac{\sigma_{\max} + \sigma_{\min}}{2} + \frac{1}{E} \cdot \bar{b} \cdot \frac{\sigma_{\max} - \sigma_{\min}}{2} \cdot \cos 2\beta \qquad \text{(Eq.1)}$$

The calibration constants $\bar{a}$ and $\bar{b}$ are based on finite element calculations and are dependent on type of hole geometry (through-hole or blind hole), on rosette geometry, on hole diameter and on depth, but not on the material. The ASTM E837-08 [10] provides these calibration coefficients for three types of Vishay Micro-Measurement Rosettes [12].

4.1 Test Specimen

The sample is a joint of the tubular truss beam, tested under fatigue loading but not cracked, as described in section 3.
The mechanical properties of the ferritic C-Mn steel of grade S355 J2 H, composing the Circular Hollow Section (CHS) joints, are presented in table 1.

Young's modulus E (N/mm^2)	Poisson's ratio	Yield stress (N/mm^2)	Tensile strength (N/mm^2)	Elongation %
210000	0.3	355	Min 470 Max 630	22

Table 1: S355 mechanical properties

The full penetrated weld was made by using the Flux cored metal-arc welding process (MAG process 136). For each joint, seven weld passes from the crown heel to the crown toe were produced (see Figure 3). The process specifications are summarised in table 2.

Electrode wire type	Current (A)	Arc voltage (V)	Travel speed (cm/min)	Interpass temperatur e (°C)	Heat input q (kJ/mm)	Range of thickness (mm)
Filarc PZ 6113, diam. 1.4 mm	270	30	20	< 250	1.94	8-30

Table 2: welding specifications

4.2 Strain-gauge rosettes

In our experiments, we have used HBM® rosettes type RY61R and RY61S, as shown in Figure 6, specially designed for hole-drilling measurements. They include a drawn target in order to insure proper centering of the hole.
The RY61S rosette is round and quite similar, in dimension, to the ASTM 1/16 in. Type A rosette. The RY61R rosette is rectangular and similar to the ASTM Type

B rosette. The latter is particularly useful for making measurements in the vicinity of the weld toe.


Figure 6: HBM Hole-drilling rosettes, RY61S on the left and RY61R on the right

These rosettes present a gauge circle with a diameter D of 5.1 mm and require a small drill-hole D_0, of 1.6 mm. They have to be glued to smooth surfaces which have initially been sandpapered.

4.3 Hole-Drilling Instrumentation

According to ASTM E837-08 [10], the hole-drilling method is designed for flat surface areas, such as plates. Even though, one can find in the literature residual stress measurements on curved surfaces (range of curvature radius from 300 to 500 mm) made by hole drilling [5], it was not possible to order a suitable drilling instrumentation to make measurement on our tubular components because of their curved surface and because of the narrow gap (g=38 mm) at the weld joint area, as can be seen on Figure 3.
As a consequence, we have developed our own drilling system shown in Figure 7, convenient for the chord diameter of 168.3 mm and allowing measurement in the edge of the weld in spite of the small distance between the braces.

The drilling system is composed of:

- A half-ring clamping support system that ensures the stability of the device and facilitates attachment on curved surfaces.
- An optical **microscope** which allows alignment of the drill bit on the rosette target, in order to keep eccentricity of the hole within tolerances (± 0.004 D, in our case ± 0.02 mm).
- Screws set on the device to adjust position in directions X, Y and Z.
- An electric **turbine** which replaces the microscope once this drill-position has been found. The drilling speed of 80000 rpm is sufficient to prevent machining-induced residual stresses in the hole-area because carbon steel is not as sensible as stainless steel or nickel alloys.

Special tungsten carbide end mills, with a 1.6 mm diameter are used with this turbine because they are suitable for HBM RY61 strain-gauge rosettes. However, this kind of end mill lasts up to three holes of approximately 1.6 mm depth before it breaks, what we have verified experimentally on the S355 steel.

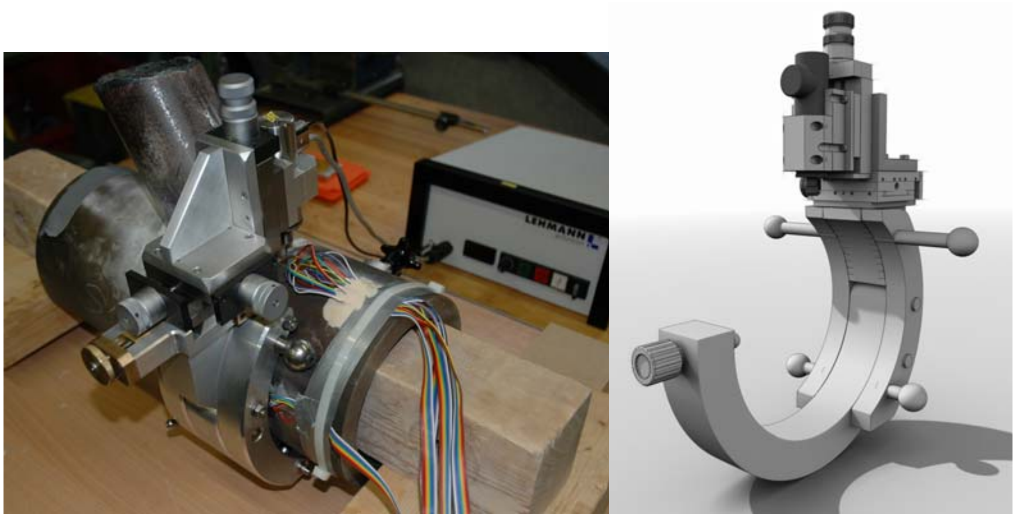

Figure 7: Hole-drilling device developed at ICOM

4.4 Calibration experiment

In order to appreciate the accuracy of the calibration constants $\bar{a}$ and $\bar{b}$ for blind-hole analysis and the reproducibility of the results, a calibration test was performed. A brace piece of the truss-beam, seen in section 3, were chosen for this test in order to keep the same material. The brace has a Circular Hollow Section of 88.9 x 8 mm.

This specimen, equipped with two rosettes RY61S and one RY61R, was loaded under a tension force increasing from 0 to 140 kN, inducing uniform tensile stress σ_c smaller than one third of the yield stress.

The rosettes were glued in such a way that directions 3 and 1 (see Figure 5) concord with the tensile stress direction and its perpendicular direction.

Figure 8: Calibration testing set-up

The calibration procedure consists in measuring the rosette strains, once before drilling the hole (under the tension force) and finally after drilling a 2 mm deep hole (under the same tensile force). The hole was drilled without loading, and the strains recorded during this operation were removed.

With the strain differences, it is possible to calculate the calibration constants as follows (Eq.2):

$$\varepsilon_{c1} = \varepsilon_{after1} - \varepsilon_{before1} \qquad \bar{a} = -\frac{2E}{1+\nu} \cdot \frac{\varepsilon_{c1} + \varepsilon_{c3}}{2\sigma_c}$$

$$\varepsilon_{c3} = \varepsilon_{after3} - \varepsilon_{before3} \qquad \bar{b} = -2E \cdot \frac{\varepsilon_{c1} - \varepsilon_{c3}}{2\sigma_c} \qquad \text{(Eq.2)}$$

The calibrating results, for one of the RY61S rosette, are plotted in Figure 9.

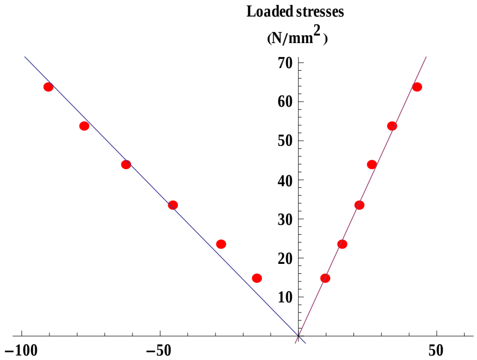

Figure 9: Stresses loaded versus calculated stresses

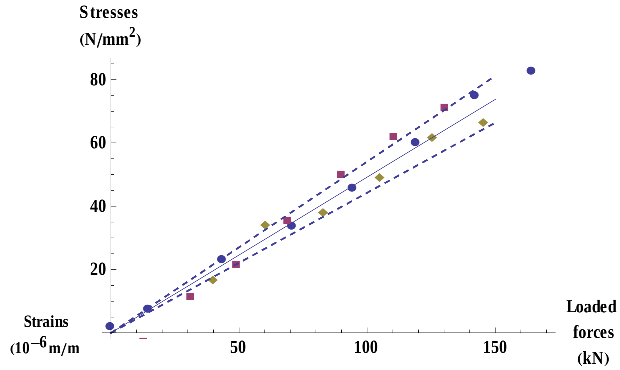

Figure 10: Loaded stresses versus measured strains

We obtained the following coefficients $\bar{a}$ and $\bar{b}$ for calibration, which we can compare to those given by the ASTM E837-8 [10] recommendations for uniform stress evaluations:

$$\bar{a}_{cal} = 0.119 \qquad \bar{a}_{ASTM} = 0.128$$

$$\bar{b}_{cal} = 0.426 \qquad \bar{b}_{ASTM} = 0.338$$

The difference for $\bar{b}$ is not negligible. It can be partially explained by the fact that, despite their similarity in geometry, the ASTM coefficients have been calibrated for Vishay Micro-Measurement Rosettes and not for HBM Rosettes.
However, if we calculate the relieved stresses using ASTM coefficients (all symbols in Figure 10) and we compare results with stresses from our loading represented as a line, for the three tested rosettes, we find that calculated stresses are within ± 10 % of the ideally expected stresses. For the hole drilling method, this can be acceptable.
After the drilling, it was noticed that the drilled hole was a little bit larger than 1.6 mm, between 1.65 and 1.75mm in our test. The residual strains recorded during the hole-drilling process were not negligible.

4.5 Residual stress measured in a K-joint

Hereafter, the first weld-induced residual stresses measured by means of our drilling device, on a non-cracked joint, are presented.
Residual stresses are measured, due to relaxation from a 2 mm deep hole, with an increasing distance from the weld toe. Three points of measurement are drilled on each side of the attached brace and residual stresses are calculated by means of uniform stress method. In Figure 12, transverse residual stresses (hoop stresses) are represented by circular symbols and longitudinal residual stresses (axial stresses) by cross symbols. An envelope for these data is then plotted, corresponding to the fitted

Figure 11: Joint 4

distribution of the mean values data set ± the standard deviation.

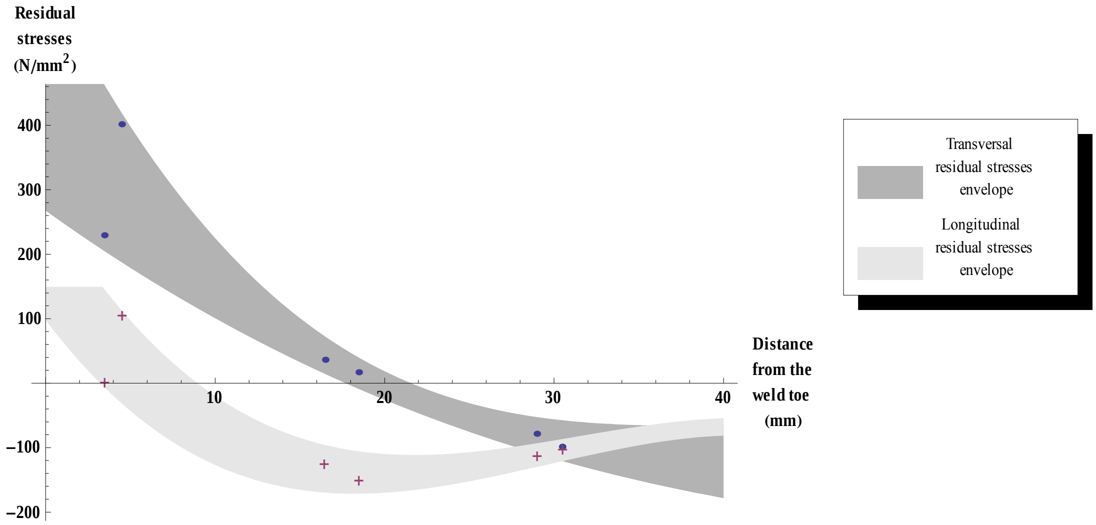

Figure 12: Transverse and longitudinal measured residual stresses in function of the distance

In Figure 13, the residual stress distribution of butt welds in pipes reported in [13] is plotted along with the previous envelopes on our welded K-joint. Leggatt, in [13], has shown the similarity between residual stresses calculated with the theory of the elastic behaviour of thin cylinders and those measured by the hole drilling method on a circumferential butt weld of a 600mm diameter pipe.

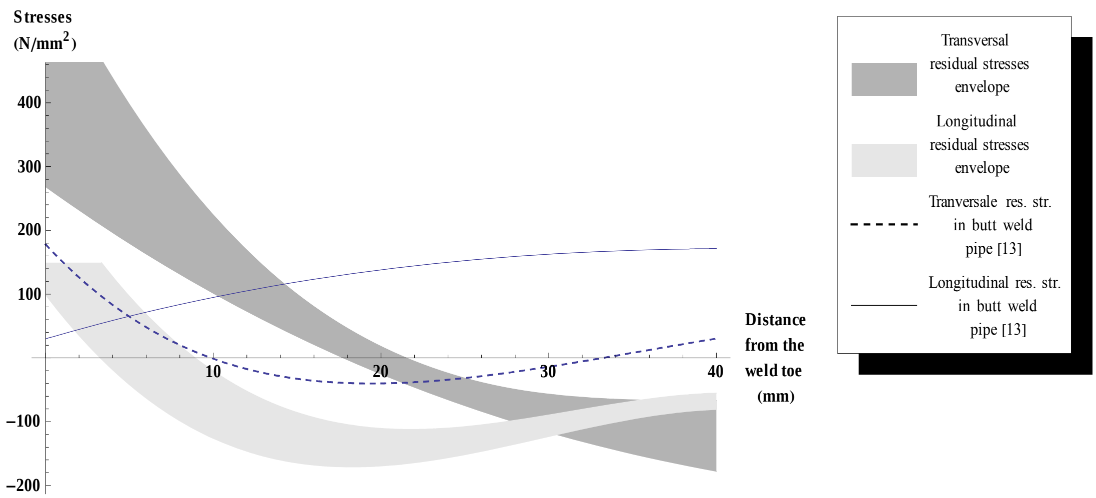

Figure 13: Comparison between [13] and measured residual stresses

Figure 13 shows that, although longitudinal residual stresses are greater than transversal ones in the vicinity of thin cylinders pipe welds, this is not the case for thick cylinders such as bridge tubular K-joints. Moreover, transversal residual stresses in these kind of joints, could exceed 0.6·fy. Above this value, the validity of the hole-drilling method is not guaranteed.

These results deserve a deeper analysis with respect to the influence of large curvature, the use of simplified uniform stress method and the effect of residual stresses exceeding 60% of the yield stress.

5 CONCLUSIONS AND FUTURE WORK

It has been shown that the drilling system developed for tubes has given suitable results with an accuracy of 10% in residual stresses assessment. In this measurement campaign, the effective hole-diameter was greater than the theoretical hole-diameter, this difference was taken into account.

The first residual stress evaluations on bridge tubular joints, presented in this paper, have led to drastically different residual stress field than found in the literature on pipe and pressure vessels tubes.

In future work, influence of tube curvatures on the accuracy of the hole-drilling method, will be studied. Moreover, in order to evaluate both intensity as well as variability of the residual stresses at surface and in the depth, measurements by means of the non-destructive neutron diffraction technique, will be performed. It will give us a complete map of the triaxial stresses.

6 REFERENCES

[1] T.R. Gurney, Fatigue of Welded Structures, Cambridge Univ. Press (1979)

[2] API RP-579 Recommended Practices for Fitness-for-Service, (Jan. 2000)

[3] Structural Integrity Assessment Proc. for Europ.Ind. (SINTAP), (Nov. 1999)

[4] R.F.D. Porter Goff, J.A. Free, W.Z. Tsiagbe, Experimental Determination of Residual Stresses in Welded Tubular T-joints, Fatigue of Off. Str. (1988) 285-295

[5] A. Stacey, J.-Y. Barthelemy, R.H. Leggatt, R.A. Ainsworth, Incorporation of Residual Stresses into the SINTAP Defect Assessment Procedure, Eng Fr Mech 67 (2000) 573-611

[6] A. Schumacher, A. Nussbaumer, Experimental study on the fatigue behavior of welded tubular k-joints for bridges, Eng Str 28 (2006) 745-755

[7] A. Nussbaumer, L.A. Costa Borges, Size effects in the fatigue behavior of welded steel tubular bridge joints, Mat.-wiss. u. Werkstofftech. 39 (10) (2008) 740-748

[8] A.M. van Wingerde, D.R.V. van Delft, J. Wardenier, J.A. Packer, Scale Effects on the Fatigue Behaviour of Tubular Structures, WRC Proc. (1997)

[9] J. Mathar, Determination of Initial Stresses by Measuring the Deformation Around Drilled Holes, ASME 56, 4, (1934) 249-254

[10] ASTM 2008, Determining Residual Stresses by Hole-Drilling Strain-Gage Method, ASTM Standard E837-08 (2008)

[11] J. Lu, Handbook of Measurement of Residual Stresses, Ed. CETIM, Society for Experimental Mechanics SEM, 1996

[12] Vishay Measurements Group, Measurement of Residual Stresses by the Hole Drilling Strain Gage Method, Tech Note TN-503-6, Raleigh, NC (1996)

[13] R.H. Leggatt, Residual stresses in welded structures, Int. Jour. of Pressure Vessels and Piping 85 (2008) 144-151